Microstructure evolution during electromigration in eutectic SnPb solder bumps

C.M. Lu, T.L. Shao, C.J. Yang, and Chih Chen[a)]
National Chiao Tung University, Department of Material Science & Engineering, Hsin-chu 300 Taiwan, Republic of China

(Received 12 January 2004; accepted 3 May 2004)

A technique has been developed to facilitate analysis of the microstructural evolution of solder bumps after current stressing. Eutectic SnPb solders were connected to under-bump metallization (UBM) of Ti/Cr-Cu/Cu and pad metallization of Cu/Ni/Au. It was found that the Cu_6Sn_5 compounds on the cathode/chip side dissolved after the current stressing by 5×10^3 A/cm^2 at 150 °C for 218 h. However, on the anode/chip side, they were transformed into $(Ni_x,Cu_{1-x})_3Sn_4$ in the center region of the UBM, and they were converted into $(Cu_y,Ni_{1-y})_6Sn_5$ on the periphery of the UBM. For both cathode/substrate and anode/substrate ends, $(Cu_y,Ni_{1-y})_6Sn_5$ compounds were transformed into $(Ni_x,Cu_{1-x})_3Sn_4$. In addition, the bumps failed at cathode/chip end due to serious damage of the UBM and the Al pad. A failure mechanism induced by electromigration is proposed in this paper.

I. INTRODUCTION

Flip-chip technology has become one of the most important packaging methods in IC packaging. One of its advantages is that a large number of very small solder bumps can be fabricated into an area array on a chip as input/output (I/O) interconnections. To meet the performance requirements, the I/O number keeps increasing. Thus the size of the bumps progressively shrinks, and electromigration has become an important reliability issue for flip-chip packages.[1,2]

Eutectic SnPb solder has been adopted for the interconnection due to its low melting point and excellent mechanical properties. Nevertheless, because of its low melting point, the flip-chip SnPb bumps can fail at the stressing condition of 5×10^3 A/cm^2 at 150 °C.[3] Therefore, electromigration behavior of eutectic SnPb solder on various UBM has been studied.[4–8] In addition, electromigration failure mechanism has been proposed.[7,8] Due to smaller opening on the chip side of the flip-chip bump, the failure occurs predominantly in the chip side. Thus the under-bump metallization (UBM) on the chip side plays an important role in the electromigration failure. However, the microstructure evolution for the SnPb solder on the Cr/Cr-Cu/Cu UBM at the failure site during the stressing process is still unclear. Furthermore, all the previous studies used cross-sectional observation, which can observe only part of the contact openings. In this study, the plan-view technique was used to examine the microstructure of the contact openings, which enables the panoramic observation of the contact openings of the chip side and substrate side. Thus it provides better understanding of the microstructure evolution during current stressing and of the electromigration failure mechanism.

II. EXPERIMENTAL

Flip-chip packages of eutectic SnPb solder bumps were prepared as described next. The UBM consisted of 0.7-μm Cu, 0.3-μm Cr-Cu, and 0.1-μm Ti. Eutectic SnPb solder paste was printed and deposited on the UBM of the wafer. Then the wafer was reflowed in a nitrogen atmosphere oven with a 210 °C peak temperature, remaining above the liquidus temperature for approximately 60 s. By sawing the wafer, individual bumped-die samples were fabricated. To fabricate flip-chip joints, the bumped die was first mounted on a BT substrate to form a flip chip, in which eutectic SnPb solder paste was printed through a metal stencil onto the metallization pads. The flip-chip sample was then reflowed for the second time in a nitrogen atmosphere oven with a 210 °C peak temperature and remained above the liquidus temperature for approximately 60 s. Finally, the flip-chip package was underfilled.

Figure 1(a) shows the cross-sectional schematic of a flip-chip bump. The metallization pad on the substrate consisted of 0.025-μm Au, 5-μm electroless Ni(P), and 20-μm Cu. Figure 1(b) shows the cross-sectional

[a)]Address all correspondence to this author.
e-mail: chih@cc.nctu.edu.tw
DOI: 10.1557/JMR.2004.0305

 © 2004 Materials Research Society

CAMBRIDGE JOURNALS
http://journals.cambridge.org Downloaded: 28 Apr 2014 IP address: 140.113.38.11

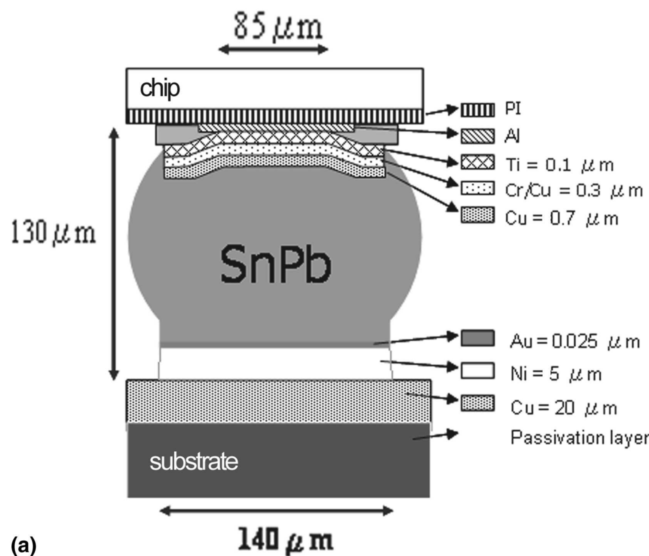

(a)

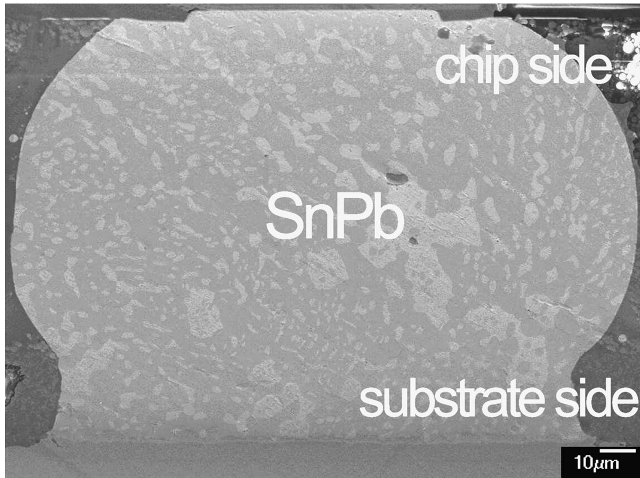

(b)

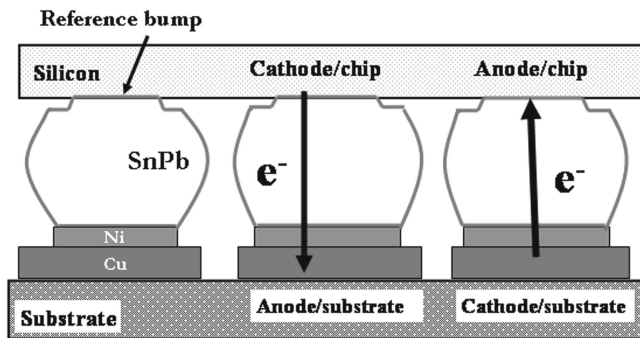

(c)

FIG. 1. (a) Schematic of a SnPb solder bump used in this study. (b) Cross-sectional SEM image of an as-prepared SnPb solder bump. (c) Plan-view of the stressing circuit on the chip side and on the substrate side. The directions of electron flow are marked by the arrows.

scanning electron microscopy (SEM) image of an as-fabricated solder bump. SnPb bump pairs in the package were stressed by a direct current current of 0.28 A at 150 °C, which corresponded to a current density of 5 × 10^3 A/cm^2. The die size was 9.5 mm × 6.0 mm with a 105-μm UBM diameter. The cross-sectional schematic diagram of the stressing circuit is depicted in Fig. 1(c). The Al trace on the chip side was 40-μm wide and 1.5-μm thick. The directions of electron flow during electromigration test are indicated by arrows. The calculated current density was based on the contact opening of the chip side, which was 85-μm in diameter. The contact opening on the substrate side was 140-μm in diameter, resulting in a smaller current density than that on the chip side. In addition, the reference bump [as shown in Fig. 1(c)] went through a similar thermal history without current stressing. Thus it was used to differentiate the morphology change due to thermal aging only.

To observe the microstructural evolution of the eutectic SnPb bumps after current stressing, both cross-sectional and plan-view observations were performed in this study. To prepare the plan-view specimens for observation by scanning electron microscope (SEM), samples were ground either from the substrate side or the chip side until there was about 10-μm thickness of solder left. Then, an etching solution consisting of glycerin, nitric acid, and acetic acid (at the ratio of 1:1:1) was used to selectively etch tin. Thus, the morphology of the intermetallic compound (IMC) and the overall contact opening can be observed clearly after the selective etching. Several bump pairs from different modules were used in this study. Some of them were observed from cross-sectional views, while the others were prepared for plan-view observations. Microstructure and composition were examined by a Joel 6500 field SEM and energy dispersive spectroscopy (EDS), respectively.

III. RESULTS AND DISCUSSION

A. Microstructure evolution during current stressing

Figure 2(a) shows the plan-view SEM image of the IMC formed on the chip side after the removal of the SnPb solder. The circle-like area with scallop-like IMCs represents the contact opening in the chip side. The IMCs were analyzed to be Cu_6Sn_5. The Cu_3Sn layer may be very thin, lying underneath the Cu_6Sn_5 IMC. Figures 2(b) and 2(c) show the magnified images of the square area A and B in Fig. 2(a) respectively. Numerous tiny particles were found on the surface of the Cu_6Sn_5 IMCs, as seen in Fig. 2(b). Surprisingly, EDS results show that the tiny particles contained Au. These might be Au-Sn IMCs, in which the Au atoms diffused from the metallization layer in the substrate during the second reflow for the package fabrication process. A rod-type IMC was also observed, as indicated by the arrow in Fig. 2(c). It was identified to be $(Cu_y,Ni_{1-y})_6Sn_5$, in which a small percentage of Ni was dissolved into Cu_6Sn_5. Because there are no Ni atoms in the UBM of the chip side and in the solder, the Ni

CAMBRIDGE JOURNALS
http://journals.cambridge.org Downloaded: 28 Apr 2014 IP address: 140.113.38.11

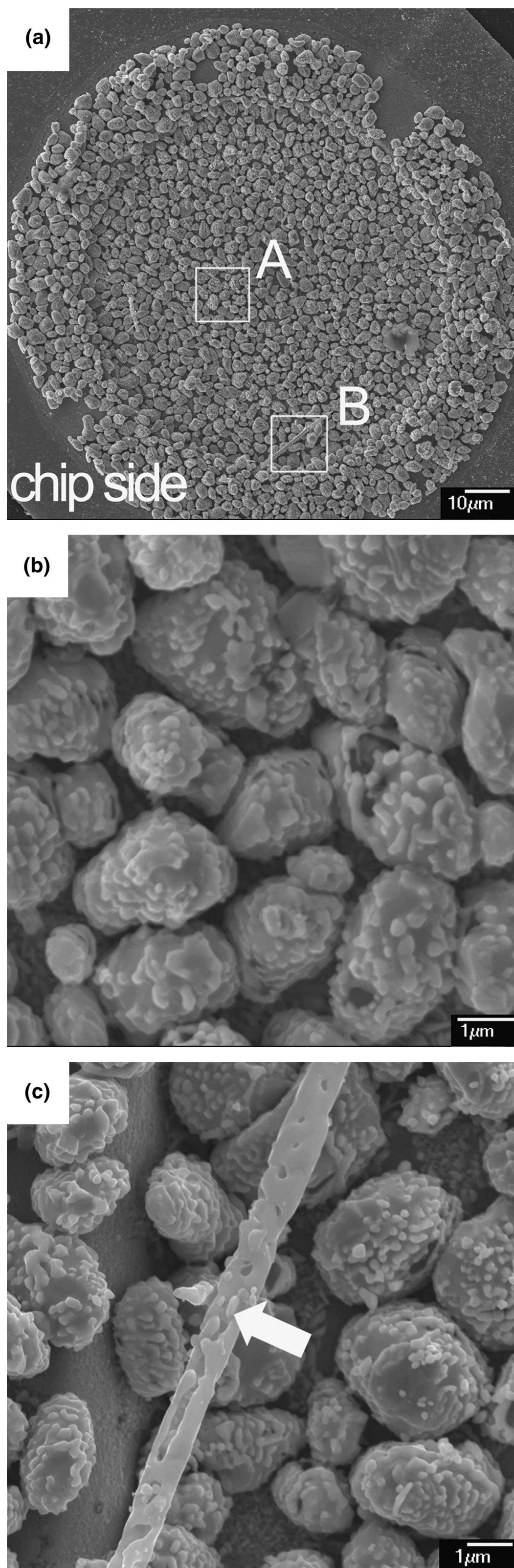

FIG. 2. Plan-view SEM images showing IMC morphology on the chip side (a) Panoramic view of the contact opening and Cu_6Sn_5 IMCs. (b) Magnified SEM image the rectangle area in (a). (c) Enlarged SEM image of IMC of the rectangular area in (a). The rod-type IMC indicated by the arrow is $(Cu_y,Ni_{1-y})_6Sn_5$, in which a small percentage of Ni atoms was detected.

atoms may diffuse from the substrate side during the second reflow for the package-fabrication process.

On the other hand, the initial IMC morphology on the substrate side is quite different from the IMC on the chip side, as seen in Fig. 3(a), which shows the contact opening on the substrate side. The enlarged SEM image of the IMC is seen in Fig. 3(b). The rod-type IMCs are identified to be $(Cu_y,Ni_{1-y})_6Sn_5$. Because there is no Cu in the metallization pad on the substrate, it is speculated that the Cu atoms diffuse from the chip side during the second reflow process.

Phase transformation of IMCs occurred in the bumps after stressing by 5×10^3 A/cm^2 at 150 °C for 218 h. The

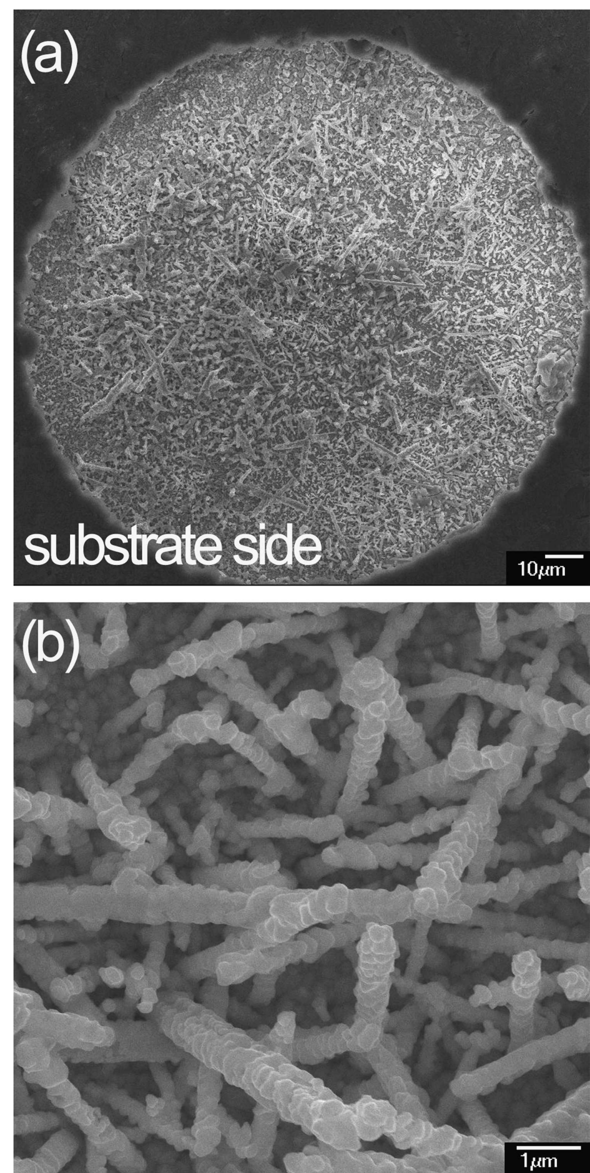

FIG. 3. Plan-view SEM images showing IMC morphology on the substrate side. (a) Panoramic view of the contact opening and $(Cu_y,Ni_{1-y})_6Sn_5$ IMCs. (b) The magnified SEM image of the rectangle area in (a), showing the morphology of $(Cu_y,Ni_{1-y})_6Sn_5$ IMCs.

CAMBRIDGE JOURNALS
http://journals.cambridge.org Downloaded: 28 Apr 2014 IP address: 140.113.38.11

morphologies of IMCs on the anode/chip and the cathode/chip can be seen in Figs. 4(a) and 4(b) respectively. The measured resistance of the stressing circuit remained the same after the current stressing. Therefore, these bumps did not fail prior to microstructure examination. An extrusion was observed around the center of the UBM on the cathode/chip, while no obvious damage was found in the anode/chip side. The extrusion consisted of Ti, Cr, Cu, and Sn, which implies that the UBM and the Al pad may be damaged by the electron flow. Interestingly, the IMCs around the center of the contact opening on anode/chip side were transformed into $(Ni_x,Cu_{1-x})_3Sn_4$, and the IMCs on the peripheral of the contact were identified to be $(Cu_y,Ni_{1-y})_6Sn_5$. Furthermore, on the cathode/chip side, the Cu_6Sn_5 IMCs in the center region of the contact disappeared after the current stressing, as seen in Fig. 4(b); whereas they became $(Cu_y,Ni_{1-y})_6Sn_5$ in the peripheral of the contact. Figures 5(a) and 5(b) show the enlarged images of the square regions of 5(a) and 5(b) in Fig. 4(a), respectively. IMCs of $(Ni_x,Cu_{1-x})_3Sn_4$ and the Cr-Sn-Au layer were detected in the contact of the anode/chip end. Figures 5(c) and 5(d) show the magnified SEM images of the square regions 5(c) and 5(d) in Fig. 4(b), respectively. Cr-Sn-Au and Cr-Sn layers were left in the center of the contact, and $(Cu_y,Ni_{1-y})_6Sn_5$ IMCs remained on the periphery of the contact in the cathode/chip end.

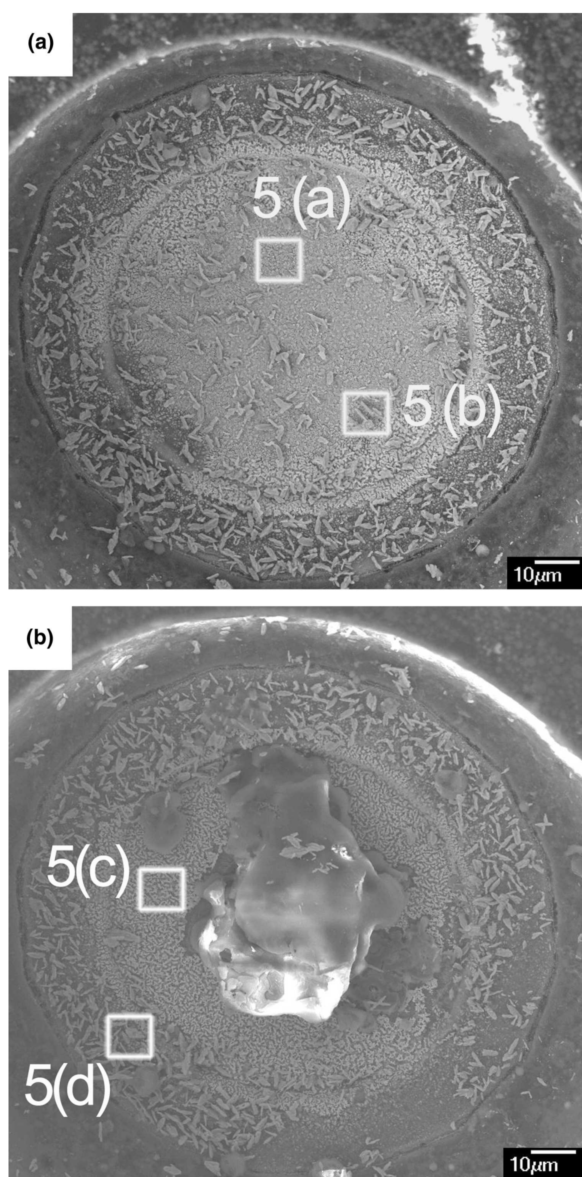

FIG. 4. Plan-view SEM images depicting the morphology of contact openings after stressing by 5×10^3 A/cm^2 at 150 °C for 218 h; (a) on the anode/chip side; (b) on the cathode/chip side. An extrusion formed on the cathode/chip side.

The evolution of IMCs, as well as their compositions before and after the current stressing, is tabulated in Table I. Because the direction of electron flow at the anode/chip end was opposite to that at the cathode/chip end, the IMC compositions on the two ends were quite different. After stressing by 5×10^3 A/cm^2 at 150 °C for 218 h, the amount of IMCs in the cathode/chip side decreased, especially in center of the contact, where most of the electrons drifted through. The electron flow may cause copper atoms to migrate from the chip to the substrate side, resulting in the dissolution of the Cu_6Sn_5 IMCs. Due to the much smaller current density in the peripheral of the contact, the IMCs in the peripheral remained. Nevertheless, their phase changed to ternary IMCs of $(Cu_y,Ni_{1-y})_6Sn_5$ with 13% nickel atoms. The Ni atoms may diffuse from the substrate side during the current stressing.

On the anode/chip side, the Cu_6Sn_5 IMCs were transformed into either $(Ni_x,Cu_{1-x})_3Sn_4$ or $(Cu_y,Ni_{1-y})_6Sn_5$ after the current stressing. In the center of the opening, ternary IMCs of $(Ni_x,Cu_{1-x})_3Sn_4$ formed, in which the weight of nickel atoms amounted to 40%. It is believed that the nickel atoms had migrated from the substrate to the chip side due to the electron flow. In addition, it is speculated that the Cu_6Sn_5 IMCs were transformed into the ternary $(Cu_y,Ni_{1-y})_6Sn_5$ IMCs first, when nickel atoms drifted to the chip side prior to failure. As nickel concentration increased, the ternary $(Cu_y,Ni_{1-y})_6Sn_5$ IMCs may have been transformed into $(Ni_x,Cu_{1-x})_3Sn_4$.[9,10] On the peripheral of the contact, ternary IMCs of $(Cu_y,Ni_{1-y})_6Sn_5$ was found, in which the weight of nickel atoms weighed comprised only 19%.

As for the reference bump, $(Cu_y,Ni_{1-y})_6Sn_5$ IMCs with 16% Ni were grown on the chip side due to the thermal aging (150 °C for 218 h) without current stressing, as seen in Table I(a). As a rough estimation, the diffusion distance for Ni atoms to diffuse in Sn matrix at 150 °C for 218 h is calculated to be 650 μm.[11] Since the bump height is approximately 130 μm, thus it is reasonable for Ni atoms to diffuse from the substrate side to the chip side after the thermal aging process. In addition, Ni atoms may also diffuse from the substrate side to the chip

CAMBRIDGE JOURNALS
http://journals.cambridge.org Downloaded: 28 Apr 2014 IP address: 140.113.38.11

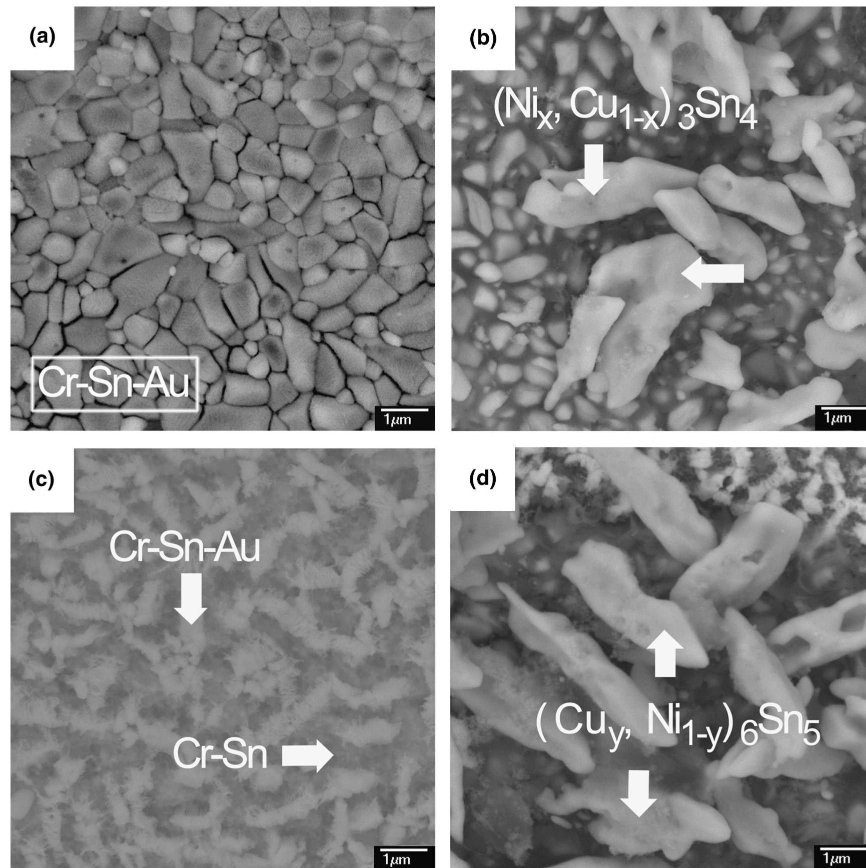

FIG. 5. Magnified SEM images of some of the area in Figs. 4(a) and 4(b). (a) Sn-Cr-Au alloy in anode/chip side, (b) $(Ni_x,Cu_{1-x})_3Sn_4$ in anode/chip side, (c) Sn-Cr and Sn-Cr-Au alloys in cathode/chip side, and (d) $(Cu_y,Ni_{1-y})_6Sn_5$ on the periphery of the contact opening at the cathode/chip side.

TABLE I. Evolution of IMC composition before and after the current stressing after stressing at 5×10^3 A/cm^2 at 150 °C for 218 h. (a) at chip side; (b) at substrate side.

(a) At chip side

Element/IMC	Before stressing (Atomic %)	After stressing (Atomic %)				Reference bump (Atomic %)
		Anode		Cathode		
		Center	Peripheral	Center	Peripheral	
Au	4 ± 1	N/D	N/D	N/A[b)]	2 ± 0	N/D
Cu	53 ± 1	2 ± 1	33 ± 1	N/A	45 ± 6	40 ± 3
Ni	N/D*	40 ± 3	19 ± 2	N/A	13 ± 1	16 ± 2
Sn	43 ± 1	58 ± 4	48 ± 1	N/A	40 ± 4	44 ± 2
IMC	Cu_6Sn_5	$(Ni_x,Cu_{1-x})_3Sn_4$	$(Cu_y,Ni_{1-y})_6Sn_5$	N/A	$(Cu_y,Ni_{1-y})_6Sn_5$	$(Cu_y,Ni_{1-y})_6Sn_5$

[a)]N/D: Not detectable.
[b)]N/A: Not available since the IMCs in the center region of the contact dissolved after current stressing.

(b) At substrate side

Element	Before stressing (Atomic %)	After stressing (Atomic %)		Reference bump (Atomic %)
		Anode	Cathode	
Au	N/D	N/D	N/D	N/D
Cu	45 ± 1	15 ± 3	13 ± 1	33 ± 5
Ni	12 ± 1	31 ± 0	31 ± 1	22 ± 5
Sn	43 ± 1	54 ± 3	56 ± 2	45 ± 0
IMC	$(Cu_y,Ni_{1-y})_6Sn_5$	$(Ni_x,Cu_{1-x})_3Sn_4$	$(Ni_x,Cu_{1-x})_3Sn_4$	$(Cu_y,Ni_{1-y})_6Sn_5$

CAMBRIDGE JOURNALS
http://journals.cambridge.org Downloaded: 28 Apr 2014 IP address: 140.113.38.11

side due to the chemical potential gradient, because the ternary IMCs may have lower free energy.[10] Therefore, on the anode/chip side, electron flow enhances the diffusion of nickel atoms. However, on the cathode side, the diffusion of nickel atoms may be retarded by the opposite electron flow. In addition, according to the results on current density simulation by Paik et al., the current density in the interior of the contact is approximately 10 times larger than that in the periphery of the contact.[12] All of the current must flow into the contact and then flow out to the Al trace on the anode/chip side. Therefore, in the center of the opening, where most of the nickel atoms may accumulate due to this current crowding effect, the nickel concentration increased up to 40%; whereas it reached only 19% for the IMCs on the periphery of the contact.

On the substrate side, the $(Cu_y,Ni_{1-y})_6Sn_5$ IMCs were transformed into $(Ni_x,Cu_{1-x})_3Sn_4$ after the current stressing, as can be seen in Table I(b). Because the contact opening of the substrate side is 140 μm, the current density passing through the substrate contact was approximately one third that of the contact of chip side. Thus the influence of current stressing on the IMC formation on the substrate side was expected to be less profound than that on the chip side. At both cathode/substrate and anode/substrate ends, the transformation of $(Cu_y,Ni_{1-y})_6Sn_5$ may be attributed to the diffusion of Ni atoms from the pad metallization layer into the IMCs during current stressing. Compared with the reference bumps (22% Ni), the nickel concentration was higher in the IMCs (31%) for the stressed bumps. It is inferred that the temperature in the stressed bumps may be higher than that in the reference due to Joule heating, which caused the higher diffusion rate of nickel atom for the stressed bumps.

B. Microstructure of failure site

Electromigration failure occurred at the cathode/chip side. Figures 6(a) and 6(b) show the cross-sectional SEM

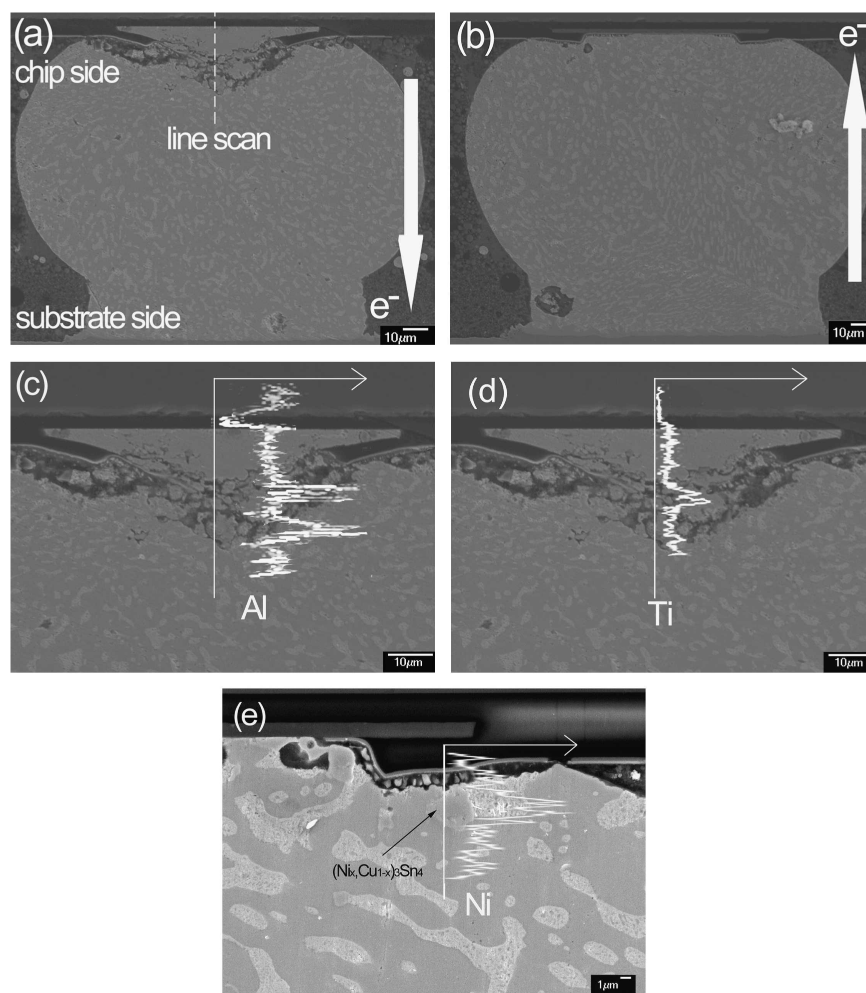

FIG. 6. Cross-sectional SEM images of bump pairs after stressing by 5×10^3 A/cm^2 at 150 °C for 216 h. (a) For the bump in which the direction of electrons drifted from chip to substrate end. (b) For the bump in which the direction of electrons was opposite to that in (a). The solder joints failed on the cathode/chip side. (c) Line-scan analysis for Al on the failed chip/cathode side. (d) Line-scan analysis for Ti on the failed chip/cathode side, showing the Al pad and that the UBM had migrated into the solder bump. (e) Line-scan analysis for Ni on the IMC near the anode/chip side.

CAMBRIDGE JOURNALS
http://journals.cambridge.org Downloaded: 28 Apr 2014 IP address: 140.113.38.11

images of the failed bump pairs after 216-h stressing by 5×10^3 A/cm^2 at 150 °C. The UBM of the cathode/chip side was seriously damaged, while there was no noticeable damage found on the anode/chip side. EDS line-scan analysis on the failure site indicates that the Al pad and the UBM had migrated into the solder bump, as seen in Figs. 6(c) and 6(d). Furthermore, solder was found to back-fill where the UBM and Al trace had been located. On the anode/chip side, numerous small voids were observed in the UBM. It is speculated that the Cu in the UBM may diffuses into the solder to form IMCs during the current stressing, leaving the voids in the UBM. Besides, $(Ni_x,Cu_{1-x})_3Sn_4$ IMCs were observed in the solder near the UBM. Figure 6(e) shows the cross-sectional SEM image for the anode/chip side. A $(Ni_x,Cu_{1-x})_3Sn_4$ IMC was observed, as indicated by the arrow in the figure. The ts composition was measured to be 31.8% of Ni, 10.5% of Cu, and 57.7% Sn. EDS line scan shows that Ni concentration in solder near the IMC was much lower than that in the IMC. No concentration gradient of Ni was detected between the substrate side and the chip side, because the solubility of Ni in the eutectic SnPb solder is less than 1% at 170 °C.[2]

To observe the failed contact opening from plan view, other pairs of solder bumps from different module were stressed by 5×10^3A/cm^2 at 150 °C, and they failed after stressing for 216 h. The SEM plan-view images for the failure site are shown in Figs. 7(a) and 7(b). Figure 7(a) shows the microstructure of the contact opening on the cathode/chip end after failure. This bump may be close to failure, but the resistance of the stressing circuit did not change. Compared with Fig. 4(b) (which depicts the microstructure of the cathode/chip end after 218-h stressing), the UBM was damaged more seriously. Cracks in the UBM were observed, and Al was detected inside the cracks. Figure 7(b) shows the microstructure on the failure site after stressing for 224 h. The UBM was severely damaged, so the circuit became open.

Therefore, it is inferred that the UBM failure induced by the electromigration in the Al trace may be responsible for the failure of the bump. Prior to the failure due to electromigration, the Cu atoms in the UBM and in the IMCs on the cathode/chip side migrated to the substrate side, so the UBM may deteriorate. Al atoms migrated into the solder, so it formed an extrusion in the weakened UBM, as seen in Fig. 4(b). Although the current density was only 5×10^3 A/cm^2 in the solder bumps, the corresponding current density in the Al trace was as high as 4.8×10^5 A/cm^2, which may have caused the migration of Al atoms from the pad into the solder. As current stressing continued, the UBM and the Al pad were damaged by the extrusion, as shown in Fig. 7(a). Besides, it is speculated that the eutectic SnPb solder near the UBM may be heated by Joule heating to over its melting point of 183 °C prior to failure. Then the Al pad and the UBM may collapse into the molten solder, as seen in Fig. 6(c); and the liquid solder may back-fill back into the place where the Al pad and the UBM had been located. After the Sn removal during the preparation process for the plan-view SEM samples, the contact opening was found to have been almost destroyed; and most of the Al pad had migrated away, as seen in Fig. 7(b). Thus the failure of the contact opening may be the reason causing the circuit failure.

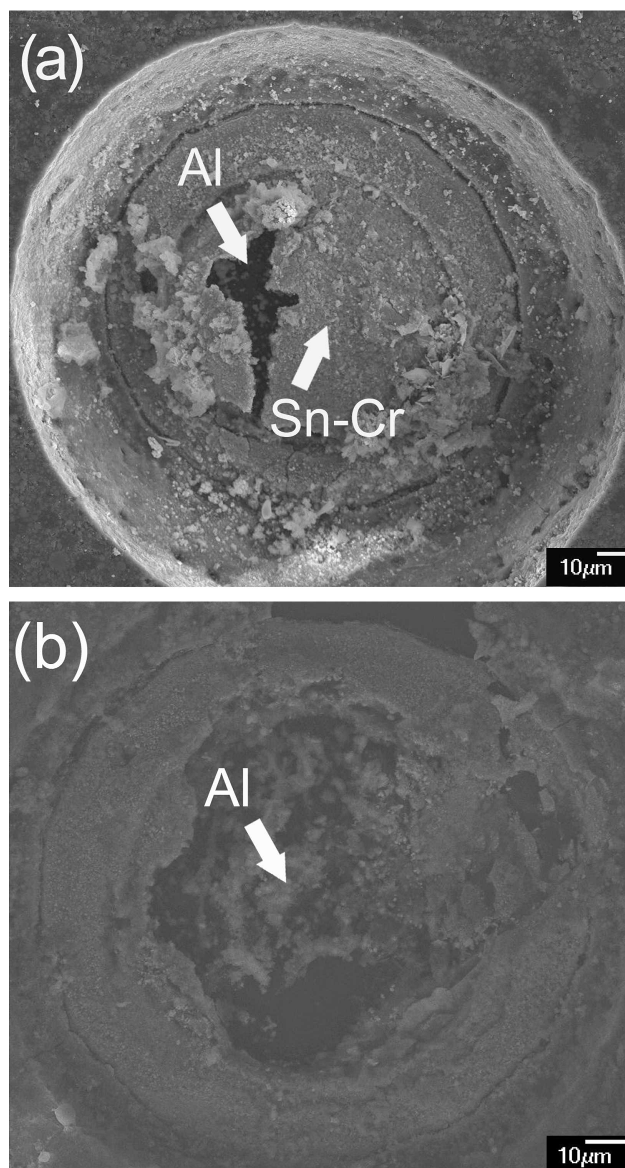

FIG. 7. Plan-view of SEM images on the cathode/chip side showing the damage caused by the electromigration under 5×10^3 A/cm^2 at 150 °C for (a) 216 h, (b) 224 h.

Note that the electromigration in the Al pad/trace should be considered because the current required in the solder bumps keeps increasing. Especially, as the bump size and pitch keep decreasing, the width of the Al trace in the rerouting circuit is limited by the small pitch.

CAMBRIDGE JOURNALS
http://journals.cambridge.org Downloaded: 28 Apr 2014 IP address: 140.113.38.11

Therefore, electromigration in Al trace needs to be considered together with the electromigration in solder bumps.

IV. CONCLUSIONS

Panoramic observation of contact openings was realized by the plan-view technique, which facilitates the microstructure analysis of the IMCs grown near the UBM and pad metallization. Prior to failure, the Cu_6Sn_5 IMCs on the cathode/chip side dissolved after the current stressing by 5×10^3 A/cm^2 at 150 °C for 218 h, and an extrusion containing Ti, Cr, Cu, and Sn was observed on the UBM. Nevertheless, on the anode/chip side, they were transformed into $(Ni_x,Cu_{1-x})_3Sn_4$ in the center region of the UBM, and they were converted $(Cu_y,Ni_{1-y})_6Sn_5$ on the periphery of the UBM. $(Cu_y,Ni_{1-y})_6Sn_5$ compounds became $(Ni_x,Cu_{1-x})_3Sn_4$ for both cathode/substrate and anode/substrate ends. Upon failure, the UBM and the Al pad/trace on the cathode/chip side had been severely damaged to become open, which was believed to be responsible for the electromigration failure.

ACKNOWLEDGMENTS

The authors would like to thank the helpful comments from Professor K.N. Tu in UCLA and the financial support by the NSC under Grant 90-2216-E-009-042.

REFERENCES

1. K.N. Tu: Recent advances on electromigration in very-large-scale-integration of interconnects. *J. Appl. Phys.* **94,** 5451 (2003).
2. K.N. Tu and K. Zeng: Tin-lead (SnPb) solder reaction in flip chip technology. *Mater. Sci. Eng. Rep.* **R34,** 1 (2001).
3. S. Brandenburg and S. Yeh: Electromigration studies of flip chip bump solder joints, Proceedings of Surface Mount International Conference and Exhibition, SM198, San Jose, CA, Aug. 23–27, 1998 (Edina, MN: SMTA, 1998), p. 337.
4. J.D. Wu, P.J. Zheng, and C.T. Kelly Lee: Chiu, and J.J. Lee: Electromigration Failures of UBM/Bump Systems of Flip Chip Packages. 2002 Electronic Components and Technology Conference, p. 452.
5. T.Y. Lee, K.N. Tu, S.M. Kuo, and D.R. Frear: Electromigration of eutectic SnPb solder interconnects for flip chip technology. *J. Appl. Phys.* **89,** 6, 3189 (2001).
6. S.Y. Jang, J. Wolf, W.S. Kwon, and K.W. Paik: UBM (under bump metallization) study for Pb-free electroplating bumping: Interface reaction and electromigration. 2002 Electronic Components and Technology Conference, p. 1213.
7. Hua Ye: Cemal Basaran, and Douglas Hopkins: Thermomigration in Pb-Sn solder joints under joule heating during electric current stressing. *Appl. Phys. Lett.* **82,** 7 (2003).
8. W.J. Choi, E.C.C. Yeh, and K.N. Tu: Electromigration of Flip Chip Solder Bump on Cu/Ni(V)/Al Thin Film Under Bump Metallization. 2002 Electronic Components and Technology Conference, p. 1201.
9. S.W. Chen, C.M. Chen, and W.C. Liu: Electric current effects upon the Sn/Cu and Sn/Ni interfacial reactions. *J. Electronic Mater.* **27,** 1193 (1998).
10. W.T. Chen, C.E. Ho, and C.R. Kao: Effect of Cu concentration on the interfacial reactions between Ni and Sn-Cu solders. *J. Mater. Res.* **17,** 263 (2002).
11. H. Mehrer: Reference database for diffusivities. (Landolt-Bönstein, New Series Group III, Vol. **26,** Springer, Berlin, 1990).
12. J.W. Nah, K.W. Paik, J.O. Suh, and K.N. Tu: Mechanism of electromigration-induced failure in the 97Pb–3Sn and 37Pb–63Sn composite solder joints. *J. Appl. Phys.* **94,** 7560 (2003).

CAMBRIDGE JOURNALS
http://journals.cambridge.org Downloaded: 28 Apr 2014 IP address: 140.113.38.11